Carbohydrate Polymers 156 (2017) 45–55

Contents lists available at ScienceDirect

Carbohydrate Polymers

journal homepage: www.elsevier.com/locate/carbpol

QbD based synthesis and characterization of polyacrylamide grafted corn fibre gum

Akashdeep Singh, Bhumika Mangla, Sheshank Sethi, Sunil Kamboj, Radhika Sharma, Vikas Rana*

Pharmaceutics Division, Department of Pharmaceutical Sciences and Drug Research, Punjabi University, Patiala 147002, India

ARTICLE INFO

Article history:
Received 19 July 2016
Received in revised form 23 August 2016
Accepted 26 August 2016
Available online 31 August 2016

Keywords:
Polyacrylamide corn fibre gum
Grafted copolymer
Mucoadhesion
Liquid like viscous gum
Rheology

ABSTRACT

The aim of present investigation was to utilize quality by design approach for the synthesis of polyacrylamide corn fibre gum (PAAm-*g*-CFG) from corn fibre gum (CFG) by varying concentration of acrylamide and initiator. The spectral analysis (ATR-FTIR, ^{1}H NMR, DSC, X-ray and Mass spectroscopy) was conducted to assure grafting copolymerization of CFG with acrylamide. The powder flow properties confirm the porous nature of PAAm-*g*-CFG. The grafted copolymer dispersion showed shear thinning behaviour that follows Herschel Bulkley model. The viscoelastic analysis suggested viscous liquid like nature of PAAm-*g*-CFG and its viscosity increases with increase in concentration of PAAm-*g*-CFG. The mucoadhesive strength of synthesized PAAm-*g*-CFG was found to be higher than moringa oleifera gum, karaya gum, guar gum, xanthan gum, chitosan and gelatin. Further, the results pointed toward enhanced thermal stability of PAAm-*g*-CFG. Thus, PAAm-*g*-CFG has a great potential to be used in food and pharmaceutical industry.

1. Introduction

Amongst natural polymers, polysaccharides are the materials of choice for drug delivery. This may be due to their biodegradability, safety, cheap, biocompatibility and easy availability from agricultural resources. However, the biodegradability reduces their shelf life and thus needs modifications (Durcilene, Regina, & Judith, 2007). Further, some previous research highlighted the wide range benefits of vinyl and other monomer based synthetic polymers. Therefore, most of the research these days aimed to utilize this power of grafting techniques. In addition, graft copolymerization contributes hydrophobic character and add stearic bulkiness, which considerably protects carbohydrates backbone that results in increase solution viscosity, improve flocculation efficiency, retard drug release, decolorize textile dyes, enhance the shear stability, impart resistance to biological degradation and super adsorbent property (Jiang et al., 2006; Mishra, Bajpai, & Pandey, 2006; Mundargi, Patil, & Aminabhavi, 2007; Singh, Tiwari, Tripathi, & Sanghi, 2004; Sanghi, Bhattacharya, & Singh, 2006; Toti & Aminabhavi, 2004). This probably the reason for the efforts made to achieve best possible graft copolymer onto the polysaccharide backbone like guar gum (Singh et al., 2004), acacia gum (Toti & Aminabhavi, 2004), cassia tora gum (Sharma, kumar, & Soni, 2002), tamarindus indica mucilage (Mishra, Bajpai, Pal, Agrawal, & Pandey, 2006), kundoor mucilage (Mishra & Bajpai, 2005), xanthan gum (Behari, Pandey, Kumar, & Taunk, 2001), carboxymethyl cellulose (Tame et al., 2011), Sodium alginate (Kurkuri, Kumbar, & Aminabhavi, 2002), amylopectin (Adhikary & Krishnamoorthi, 2013), starch (Pledger Jr., Young, Wu, Butler, & Hogen-Esch, 1986), carboxymethyl starch (Cao, Qing, Sun, Zhou, & Lin, 2002), chitosan (Al-Karawi, Al-Qaisi, Abdullah, Al-Mokaram, & Al-Heetimi, 2011), carrageenan (Darmayanti & Radiman, 2015) and cashew gum (da Silva, de Paula, & Feitosa, 2007). However, no attempt has been made to graft arabinoxylans (e.g. Corn Fibre gum).

Corn fibres are rich source of arabinoxylans (AX). Corn fibres are byproduct of corn wet and dry milling process. A part of abundantly produced corn fibres are well utilized, but remaining is left as agriculture waste. Thus, the best use of corn fibres could be to extract arabinoxylans by alkali or alkaline hydrogen peroxide solution treatments. The corn fibre contain corn fibre gum that chemically consists of a linear backbone of β-1, 4 linked xylopyranose backbone with arabinose as side chain on 2,3, or 5- linked position along with some glucuronic acid residue linked to secondary hydroxyl group of xylose residue of backbone (Yadav, Johnston, & Hicks, 2009) and galactose found as terminal residue (Yadav, Johnston, & Hicks, 2007). CFG is highly branched galactoglucuronoarabinoxy-

* Corresponding author.
E-mail addresses: vikas_pbi@rediffmail.com, vikas@pbi.ac.in (V. Rana).

http://dx.doi.org/10.1016/j.carbpol.2016.08.089
0144-8617/

lans containing only about 16–25% of total xylose in the backbone with no side chain and terminal xylose residue represent about 4–9% and remained 66–80% were substituted of total xylose residue (Yadav et al., 2007). Corn fibre gums is widely used in a variety of industrial application such as new food gum, additives in plastic, dietary fibres, polymers for chemical and pharmaceutical application because of its low cost and act as excellent emulsifier of oil-in-water emulsion system (Kamboj & Rana, 2014).

The polyacrylamide chain reaction onto corn fibre gum (CFG) probably occurs when a radical is formed in the alkoxy group of the xylopyranose monomer by abstracting hydrogen atom from the 2nd and 3rd positioned-OH moieties of β-1, 4 linked xylopyranose backbone. Grafting is expected to be initiated when acrylamide reacts with active sites of macroradical. The ammonium persulfate may induce homopolymerization when acrylamide reacts with the initiator, directly. In this reaction macroradical was formed by the reaction between sulfate radicals and hydroxyl group of the xylopyranose backbone (Maia, Silva, Curti, & Balaban, 2012).

Thus, the aim of the present investigation was to utilize quality by design approach for the synthesis of graft copolymer of corn fibre gum using acrylamide for the purpose of improving mucoadhesion and rheological performance of putative form. Therefore, the synthesized graft copolymer was examined for improved physical, rheological and spectral attributes.

2. Materials and methods

2.1. Materials

Corn fibers were procured from local flour mill, Patiala, India and corn fibre gum was extracted as per method reported by Kamboj and Rana (2014) (mol. wt. 3.18×10^5 g/mol; intrinsic viscosity 1.746 dl/g at 25 °C). Acrylamide and Sodium hydroxide was purchased from LobaChemie, India. *n*-Hexane was supplied by Merk specialities, Mumbai, India. Hydrogen peroxide solution and Hydrochloric acid were procured from Thermo Fischer scientific, India. Ammonium persulfate was obtained from s.d. fine-Chem Ltd. All other chemicals used were of analytical grade and used as received.

2.2. Method

2.2.1. Synthesis of PAAm-g-CFG

A corn fiber gum was extracted according to the method reported by Kamboj and Rana (2014). From this extracted gum, PAAm-*g*-CFG was synthesized by modifying the method reported by Rani, Sen, Mishra, and Jha (2012) and Singh, Kumar, and Sanghi (2012). In brief, 2.5% w/v gum solution was prepared in water. Separately, different concentrations of 1–5 g of acrylamide (monomer) solution in distilled water were prepared as per trials shown in Table 1. This monomer solution was added drop wise to gum solution with continuous stirring for 2 h followed by addition of different amount of ammonium persulfate (initiator). This solution was microwaved at 400 MW for 30 s till solution starts boiling. This hot solution was immediately cooled in ice-cold water. This procedure was repeated for 18 cycles till gel like consistency was obtained. This solution was kept overnight in a refrigerator for 24 h. The PAAm-*g*-CFG was precipitated by the addition of acetone. The filtered precipitates were washed with methanol: water (70:30) to remove any homopolymers. The precipitated gum was lyophilized to obtain dried product.

2.2.2. Experimental design

In the present work, 3^2 full factorial design was applied on critical synthesis parameters (CSP, X_1 = concentration of monomer, X_2 = concentration of initiator) to generate design space and optimize formulation with an aim to obtain critical quality attributes (CQA, Y_1 =% grafting, Y_2 =% yield of gum, Y_3 =% grafting efficiency). Different concentration of two CSP viz., X_1 = polyacrylamide with their low (1 g), medium (3 g) and high level (5 g) and X_2 = ammonium persulfate with their low (0.2 g), medium (0.3 g) and high level (0.4 g) were selected. 3^2 full factorial design was applied using Design expert software (Version 10, Stat-ease. Inc, USA) and the polynomial equation generated was

$$Y = \beta_0 + \beta_1 X_1 + \beta_2 X_2 + \beta_{12} X_{12} + \beta_1{}^2 X_1{}^2 + \beta_2{}^2 X_2{}^2$$

Where, Y is the dependent variable, β_0 is the arithmetic mean response of the nine runs and β_i (β_1, β_2, β_{12}, β_{11} and β_{22}) is the estimated coefficient for the corresponding factor Xi (X_1, X_2, X_{12}, X_{11} and X_{22}), which represents the average results of changing one factor at a time from its low to high value. The interaction term (X_{12}) depicts the changes in the response when two factors are simultaneously changed. The polynomial terms $X_1{}^2$ and $X_2{}^2$ are included to investigate quadratic model. The magnitude of coefficients in polynomial equation have either positive sign indicating synergistic effect or negative sign indicating antagonistic effect. Best fitting experimental model (linear, two factor interaction and quadratic) was taken statistically on the basis of comparison of several statistical parameters like coefficient of variation (CV), multiple correlation coefficient (R^2), adjusted multiple correlation coefficient (adjusted R^2), predicted residual sum of square and graphically by Contour Plot, 3D response surface plot provided by Design Expert software. The level of significance was considered at p-value <0.01.

2.2.3. Grafting evaluation

The percentage grafting was calculated using formula

$$(Y_1)\,\%\,\text{grafting} = (\text{weight of graft copolymer-weight of polysaccharide})/(\text{weight of polysaccharide}) \times 100$$

$$(Y_3)\,\%\,\text{grafting efficiency} = (\text{weight of graft copolymer-weight of polysaccharide})/(\text{weight of monomer}) \times 100$$

2.2.4. pH and conductivity determination

Aqueous dispersion (1% w/v) of PAAm-*g*-CFG or its putative form was prepared and the pH along with Conductivity was determined using ESICO pH meter 1611. Sample was analysed in triplicate and results are given as the average ± standard deviation of the experimental values.

2.2.5. Zeta potential

The zeta potential of PAAm-*g*-CFG or its putative form was ascertained by using Zetasizer (Malvern instrument Ltd., UK) as reported by Kamboj and Rana (2014).

2.2.6. Powder characteristics

The powder characteristics of PAAm-*g*-CFG or its putative form [bulk and tap density, hausner ratio, compressibility index, swelling capacity and effective pore radius ($R_{effe.p}$)] was determined as per method reported by Kamboj and Rana, (2014).

2.2.7. Spectral attributes

2.2.7.1. ^1H NMR spectroscopy. High resolution ^{1}H NMR spectra were recorded on the Bruker Avance II 400 NMR spectrometer operating at spectral width of typically 12019 Hz at 25 °C. Samples were dissolved in D_20 (99%) at concentration of 15 mg/ml. The chemical shift of polysaccharide signals were determined by using the signal of water at 4.70 ppm as an internal reference (Kamboj & Rana,

Table 1
3^2 full factorial design for the synthesis of PAAm-g-CFG and its physicochemical properties.

Detail of 3^2 full factorial design

Codes	Independent Variables	Levels			Codes	Dependent variables	Low	High	Objective
		Low(-1)	Middle (0)	High(1)					
X_1	Conc of monomer (g)	1	3	5	Y_1	% Grafting	49	552	Maximum
X_2	Conc of initiator (g)	0.2	0.3	0.4	Y_2	% Yield	1.49	6.52	Maximum
–	–	–	–	–	Y_3	%Grafting efficiency	49	110	Maximum

Experimental Trials	S1	S2	S3	S4	S5	S6	S7	S8	S9
X_1	−1 (1 g)	−1 (1 g)	−1 (1 g)	0 (3 g)	0 (3 g)	0 (3 g)	1 (5 g)	1 (5 g)	1 (5 g)
X_2	−1 (0.2 g)	0 (0.3 g)	1 (0.4 g)	−1 (0.2 g)	0 (0.3 g)	1 (0.4 g)	−1 (0.2 g)	0 (0.3 g)	1 (0.4 g)
Y_1 (%)	49 ± 0.89	78 ± 1.12	103 ± 1.34	196 ± 2.12	280 ± 2.1	320 ± 1.5	395 ± 1.6	486 ± 1.7	552 ± 2.4
Y_2 (%)	1.49± 0.23	1.78 ± 0.24	2.03 ± 0.12	2.96 ± 0.41	3.8 ± 0.24	4.2 ± 0.15	4.95 ± 0.14	5.86 ± 0.36	6.52 ± 0.34
Y_3(%)	49 ± 0.49	78 ± 1.12	103 ± 1.12	65.3 ± 0.53	93.3 ± 1.4	106 ± 1.76	79 ± 1.31	97.2 ± 2.5	110 ± 2.8

Physicochemical Properties

S. No.	Polymer	pH	Conductivity (mS/cm)	Zeta Potential (mV)	Bulk density (g/cm^3)	Tapped density (g/cm^3)	Hausner ratio	Compressibity (%)	$R_{eff.p}$ (mm)	Swelling capacity
1.	PAAm-g-CFG	3.6 ± 0.2	0.807 ± 0.002	−12.4 ± 0.4	0.485 ± 0.012	0.56 ± 0.02	1.16 ± 0.03	14.2 ± 0.14	3.030 ± 12	1.8 ± 0.13
2.	CFG	7.0 ± 0.2	0.439 ± 0.004	−11.6 ± 0.3	0.54 ± 0.30	0.62 ± 0.03	1.14 ± 0.13	12.9 ± 0.14	1.99 ± 0.33	1.5 ± 0.12
3.	Required	–	–		–	–	<1.25	Below15%	Maximum	Maximum

2014). The acquisition and relaxation time were of 1.36 s and 1.0 s, respectively.

2.2.7.2. ATR-FTIR. PAAm-*g*-CFG or its putative form were identified employing ATR-FTIR spectrometer (Bruker, alpha E, Germany) in the spectral region of 500–4000 cm^{-1}. The lyophilized dry powder was used for spectral analysis.

2.2.7.3. Thermal analysis. An accurately weighed sample (about 5–10 mg) of PAAm-*g*-CFG or its putative form was placed in sealed aluminium pans, under nitrogen flown at a heating rate of 10 °C/min from 30 to 400 °C. Peak transition as well as enthalpy of fusion was estimated from the DSC131 Evo (Setaram, Lab Sys Evo, France).

2.2.7.4. X-ray diffraction. X-ray diffractogram of PAAm-*g*-CFG or its putative form were recorded employing X'pert-PRO High Resolution Powder Diffractometer (PANalyticals, Almelo, Netherlands) using copper Kα radiation generated at 40 kV and 35 mA in the differential angle range of 3–70°2θ.

2.2.7.5. Mass spectroscopy. The purified PAAm-*g*-CFG or its putative form was subjected to partial hydrolysis. In brief, sample was dissolved in 25 ml of 0.1N HCl and reflux for 1 h at 80 °C. The hydrolysate was neutralized with 1N NaOH and dialyzed for 24 h to remove excess ions. Further, mass spectroscopy of PAAm-*g*-CFG was performed by the method reported by Sharma, Kamboj, Khurana, Singh, and Rana (2015)

2.2.8. Morphological analysis

Morphological features of the PAAm-*g*-CFG or its putative form were studied with a scanning electron microscope (Joel JSM-6610 LV, Tokyo, Japan). The PAAm-*g*-CFG powder sample was mounted on a metal stub and sputtered with gold in order to make the sample conductive and the images were taken at an accelerating voltage of 10 KV and at varied magnification.

2.2.9. Gel strength

The gel strength was determined as per method reported by Jindal, Rana, Kumar, Sapra, and Tiwari, (2013). The experiments were performed using a TA XT Plus Texture Analyzer (Stable Micro Systems Ltd., Godalming, U.K.) equipped with a 300 N load cell. For performance of back extrusion tests, a rig (model A/BE, Stable Micro Systems) was used consisting of a flat 35 mm diameter perspex disc plunger that was driven into a larger perspex cylinder sample holder (50 mm diameter) to force down into the different concentrations of PAAm-*g*-CFG or its putative form (5–10% w/v) and flow it upward through the concentric annular space between plunger and the container. The measuring cup was filled with 30 ± 1 ml of different concentrations of PAAm-*g*-CFG or its putative form. The test was replicated eight times at a pretest speed of 1.0 mm/s, test speed of 2.0 m/s at a distance of 50 mm above the top of the sample, penetrated to a depth of 10 mm and returned to starting position. The cone penetration test was performed using spreadability rig (HDP/SR, Stable Micro Systems). It consisted of a 45° conical perspex probe (P/45C) that penetrated a conical sample holder containing 5 ± 0.1 ml of the different concentrations of PAAm-*g*-CFG or its putative form (5%, 8%, 10% w/v). Samples were penetrated to a distance of 50 mm at 3 mm/s compression rate. The work of shear (Ns) and firmness (N) were calculated.

2.2.10. Mucoadhesive strength

The physical mixture of CFG or PAAm-*g*-CFG was grinded with mortar and pestle. This mixture was compressed separately employing a 13 mm diameter die on an infrared hydraulic press using compression forces 100 kg/m^2 for 3 min.

The porcine gastric mucosa or mucin solution (2% w/v in PBS pH 7.4) was used as the model mucoadhesive for the estimation of ex-vivo mucoadhesive strength. The mucosal membrane was excised by removing the underlying connective tissue placed on the base of texture analyser probe and probe was filled with simulated gastric fluid. Whereas, experiments in which mucin (2% w/v) solution was used, should contain cellophane sheet as model membrane placed at the base of probe. A disc of PAAm-*g*-CFG or its putative form was attached to the stainless steel probe fixed to the mobile arm of the texture analyser. The area of contact of mucosa cellophane membrane was moistened with 1 ml of simulated gastric fluid or mucin (2% w/v) solution. The mobile arm was lowered at a rate of 0.5 mm/s until a contact with the membrane was made. A contact force of 10 g was maintained for 300 s, after which the probe was withdrawn from the membrane. The peak detachment force was recorded as a measure of mucoadhesive strength.

2.2.11. Rheological performance

The rheological behaviour of corn fibre gum and PAAm-*g*-CFG was studied using MCR-52 Rheometer (Anton Paar, Germany) using parallel plate geometry PP50 (50 mm diameter) with a 0.5 mm measuring gap. Temperature was maintained by Anton Paar, peltier system. During the experiments, the shearing geometry was covered with low viscosity liquid paraffin in order to prevent water loss. The dynamic viscosities was determined by varying the shear rate (0–100 s^{-1}) at controlled shear stress and varying shear stress (0–100 Pa) at controlled shear rate keeping at 25 °C. The temperature sweep was carried out from 10 °C to 80 °C and 80 °C to 10 °C with heating/cooling rate of 2 °C/ min.

The dynamic viscoelastic behaviour of CFG and PAAm-*g*-CFG was performed at amplitude sweep level and frequency sweep level. The linear viscoelastic region (LVR) for the gelation sample was obtained from a plot of percentage strain vs loss modulus (G″)/storage modulus (G′) at amplitude sweep mode. This percentage strain in the LVR was employed for frequency sweep and a plot of G′ and G″ vs angular frequency (ω).

3. Results and discussion

3.1. QbD based synthesis of PAAm-g-CFG

Preliminary studies were conducted to screen the critical synthesis parameter and critical quality attributes. It was evident that concentration of acrylamide (X_1) and concentration of ammonium persulfate (X_2) are the only critical synthesis parameters while keeping other process parameters constant and that could significantly influenced CQA (Y_1–Y_3). Therefore, the trials for the synthesis of PAAm-*g*-CFG was conducted by employing 3^2 full factorial design to achieve optimize synthesis process. For this purpose, nine experimental runs were conducted to analyze main effect (X_1, X_2), interaction effect (X_1X_2) and quadratic effect (X_1^2, X_2^2) for two CSP on three CQA using 3^2 full factorial design. A probability value by regression analysis was found to be $p < 0.01$ with 99% confidence level indicating the significant effect of CSP on CQA. The large p value ($p > 0.05$) for lack of fit test indicates that the test is insignificant suggest that significant model correlation existed between the CSP and CQA. Further, the data obtain was analysed using Design expert Software (Version 10, Stat-ease. Inc, USA) and following equations were generated.

$$Y_1 = 278 + 200.5X_1 + 55.83X_2 + 25.75X_1X_2 + 9.12X_1^2 - 14.88X_2^2$$

($R^2 = 0.99$, Quadratic model)

$$Y_2 = 3.78 + 2.01X_1 + 0.56X_2 + 0.26X_1X_2 + 0.091X_1^2 - 0.15X_2^2$$

($R^2 = 0.99$, Quadratic model)

$$Y_3 = 92.57 + 9.37X_1 + 20.95X_2 - 5.75X_1X_2 - 3.14X_1^2 - 5.09X_2^2$$

($R^2 = 0.99$, Quadratic model)

Each of the above equation contains contribution of main effect (X_1 and X_2), interaction term (X_1X_2) and quadratic term (X_1^2 and X_2^2). The coefficient of each of the term indicates contribution of it in enhancing% grafting and % yield. The correlation of coefficient (b_1 and b_2) associated with the effect of various synthesis parameters on%grafting (X_1), % yield (X_2) and% grafting efficiency (X_3) are shown in Table 1. The negative magnitude of a coefficient means opposite effect while positive magnitude of a coefficient means augmentative effect. Thus, it could be evident from above equations that the percentage grafting and percentage yield increased with increase in concentration of acrylamide. However, the percentage grafting efficiency was increased with increase in concentration of ammonium persulfate. Further, the contribution of interaction terms was more pronounced as compared to quadratic terms. However, the role of interaction terms as well as quadratic terms was to antagonize the grafting efficiency. This was also observed from 3D response surface plot as shown in Fig. 1. A numerical optimization technique employing desirability concept was used to develop a new synthesis process with desired response. On comprehensive evaluation of feasibility search and subsequent exhaustive grid search conducted by design expert software, the optimized synthesis procedure should have 5 g acrylamide, 0.4 g of ammonium persulfate in a batch size of 7.9 g at 80 °C temperature conditions fulfilled maximum requirement of an optimized synthesis process of PAAm-*g*-CFG. This is because of better 552 ± 2.4% grafting, 6.52 ± 0.34% yield and 110 ± 2.8% grafting efficiency. The response surface plots and corresponding plots showing the effects of different concentration X_1, X_2 on desirability are shown in Fig. 1. The desirability function added all CQA in measurement and provides possibilities to predict the optimum levels of the independent variables. The predicted desirability of the optimized formulation was found to be 0.96. The magnitude of desirability near to 1 reflects the responses values are consequently nearer to targeted values. The prediction error for all the responses parameters ranges from 2.5 to 3% suggesting a good correlation of predicted vs observed responses. The scheme for the synthesis of PAAm-*g*-CFG is summarized below:

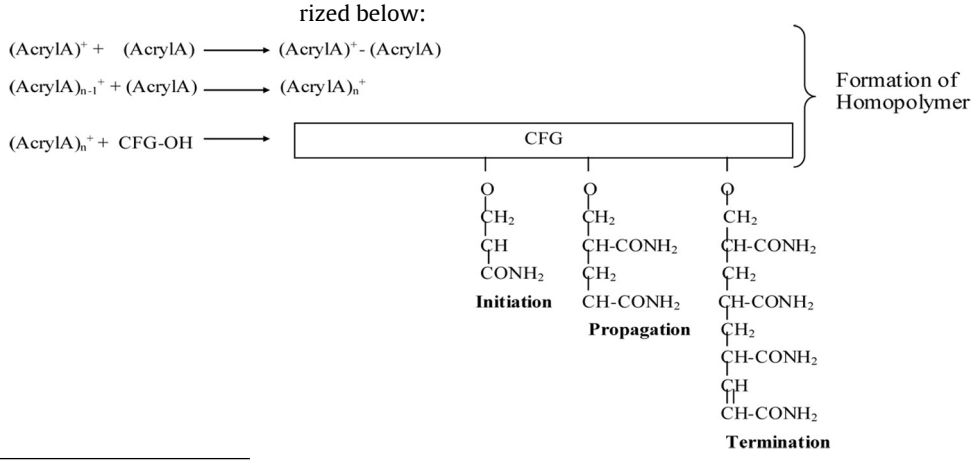

3.2. Powder characterization

The powder characteristic of PAAm-*g*-CFG suggested flowable and compressible powder similar to its putative form (Table 2). However, polyacrylamide derivatization of CFG enhances porosity as well as improves swelling characteristics.

Table 2
Mass spectroscopic analysis of PAAm-g-CFG.

S.No.	m/z ratio	Fragment
1	9385.592	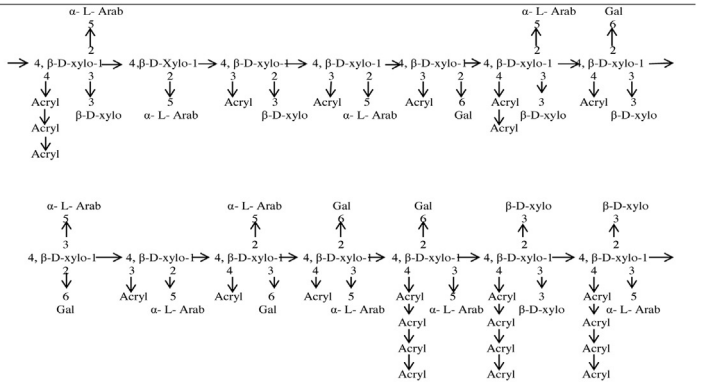
2	1462.462	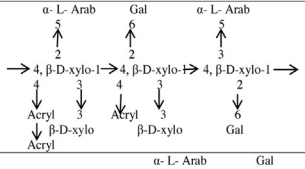
3	1330.332	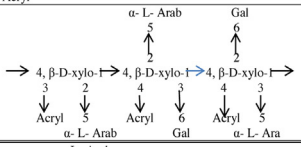
4	1209.23	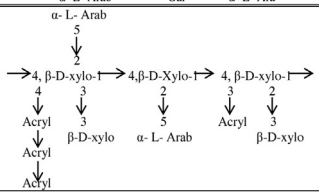
5	700.706	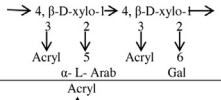
6	609.63	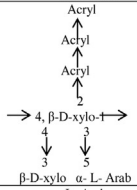
7.	467.47	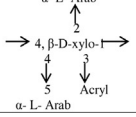

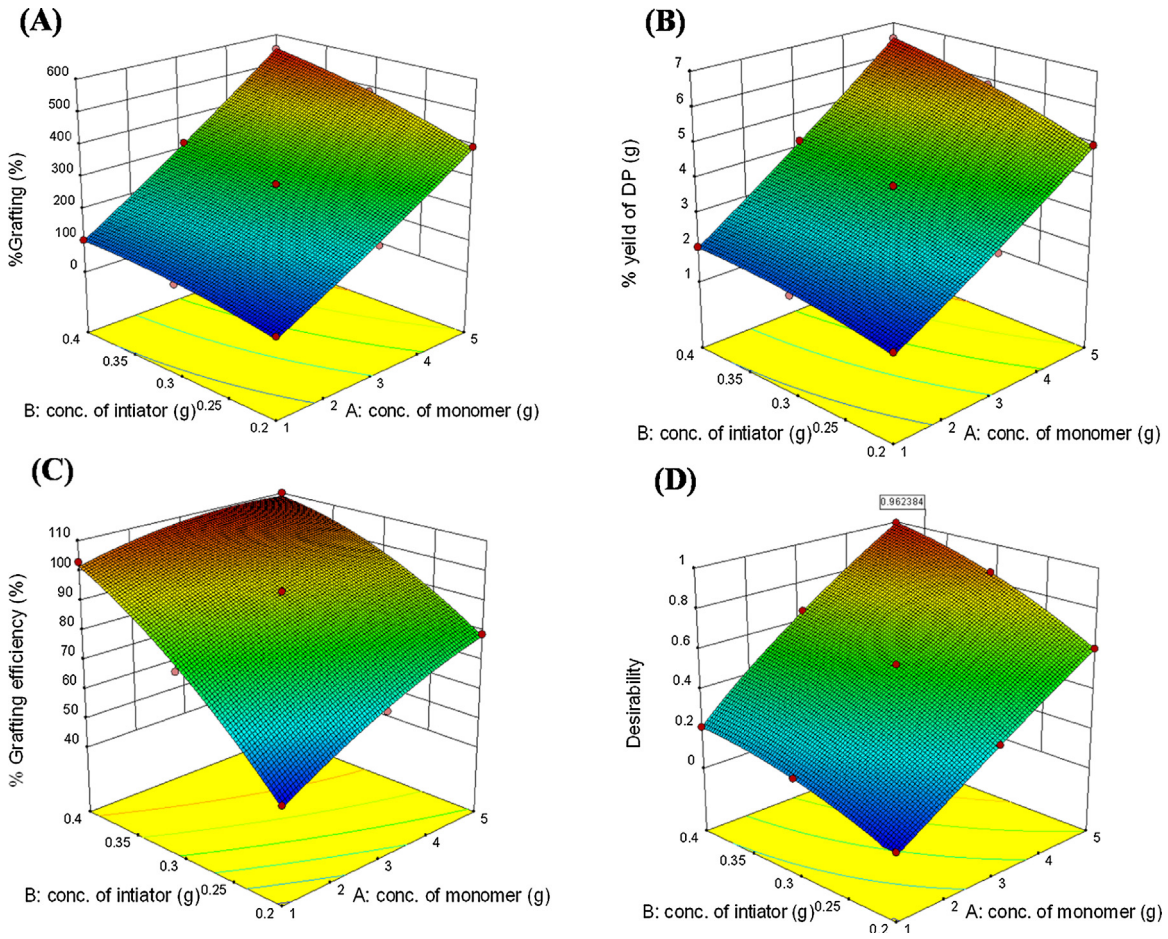

Fig. 1. 3D Response surface plot showing (A) % Grafting; (B) % Yield of DP; (C) % Grafting efficiency; (D) Desirability.

3.3. Spectral attributes

The fine structure of various water soluble AX fractions was first studied by liquid state ^{1}H NMR. Comparative studies were carried out using ^{1}H NMR of grafted gum and pure CFG to confirm the grafting of CFG backbone. ^{1}H NMR spectrum (Fig. 2A) of CFG showing peak at δ 5.34 ppm which might be from the furanoarabinose units and δ 3.42 ppm for D-glucuronic acid residue. The spectrum showing peaks at δ 3.19–4.41 ppm seems to belong to hydrogen atoms of xylose units. The peak at δ 4.219, 3.903, 4.064 ppm belongs to 2-H, 3-H, and 4-H of xylose ring. The signal at δ 3.84, 4.19, 3.38 as well as 4.06 and 3.36 ppm belongs to CH_2 group of xylose and arabinose units, respectively (Kamboj & Rana, 2014). Sample of PAAm-*g*-CFG showed additional peaks at 2.1 and 1.5 ppm (Fig. 2A) which was attributed to protons of —CH and CH_2 groups of amide, respectively in PAAm molecule (Gowrav, Umme, Hosakote, Riyaz, & Srivastava, 2015). Thus, ^{1}H NMR spectrum confirms that CFG was successfully grafted with PAAm.

The ATR-FTIR Spectra of CFG showed prominent bands corresponding to gum appears at 1645 cm^{-1}, 1516 cm^{-1} and 1012 cm^{-1}as shown in Fig. 2B. The small bands at 1341 cm^{-1}, 1253 cm^{-1}, 1147 cm^{-1} and 848 cm^{-1} indicate syringle, guaiacyl ring breathing with C=O stretching aromatic C—H in-plane deformation and aromatic C—H out of plane bending vibrations in CFG thus, showing negligible amount of lignin content in the sample. The absence of bands corresponding to 1410 cm^{-1}, 1220 cm^{-1} and 1155 cm^{-1} indicate that the extracted CFG was free from residual lignin. The appearance of sharp band at 890 cm^{-1} is characteristic peak of β-glycosidic linkage between sugar units. This suggested xylose residues forming the backbone of macromolecules are linked by β form bonds. The ATR-FTIR spectra obtained was found to be same as reported by Gupta, Madan, and Bansal (1987); Sun, Fang, Tomkinson, and Jones (1999); Xu and Sun (2004). In case of PAAm-*g*-CFG spectra, additional peak at 1602 cm^{-1}(N—H bending), 1414 cm^{-1} (C—N Stretching) and 3183 cm^{-1} due to symmetric NH stretching of NH group was observed (Fig. 2B). This confirms the successful grafting in PAAm-*g*-CFG.

The DSC thermogram of CFG showed two endothermic transitions at 89.16 °C and 231.15 °C as well as one exothermic transition at 280.31 °C (Fig. 2C). The first transition could be ascribed due to moisture/bound water present in the sample. The second endothermic peak could be due to melting of CFG sample. The first exothermic transition has arisen due to degradation of pure gum. The results were similar to those observed by Kamboj and Rana (2014). The DSC thermogram of pure PAAm-*g*-CFG (Fig. 2C) showed three endothermic transitions respectively at 82.88 °C, 160.3 °C and 281.09 °C. The first broad endotherm at 82.88 °C with heat of fusion 195.477 J/g could arise due to moisture/bound water present in the sample. The appearance of second and third endothermic transition at 160.3 °C with heat of fusion 12.27 J/g and 281.09 °C with heat of fusion 263.48 J/g could be considered as characteristic of PAAm-*g*-CFG.

The XRD spectra of PAAm-*g*-CFG are shown in Fig. 2D. The absence of diffraction peaks indicates the absence of crystallinity in PAAm-*g*-CFG which suggested the amorphous nature of both PAAm-*g*-CFG as pure CFG.

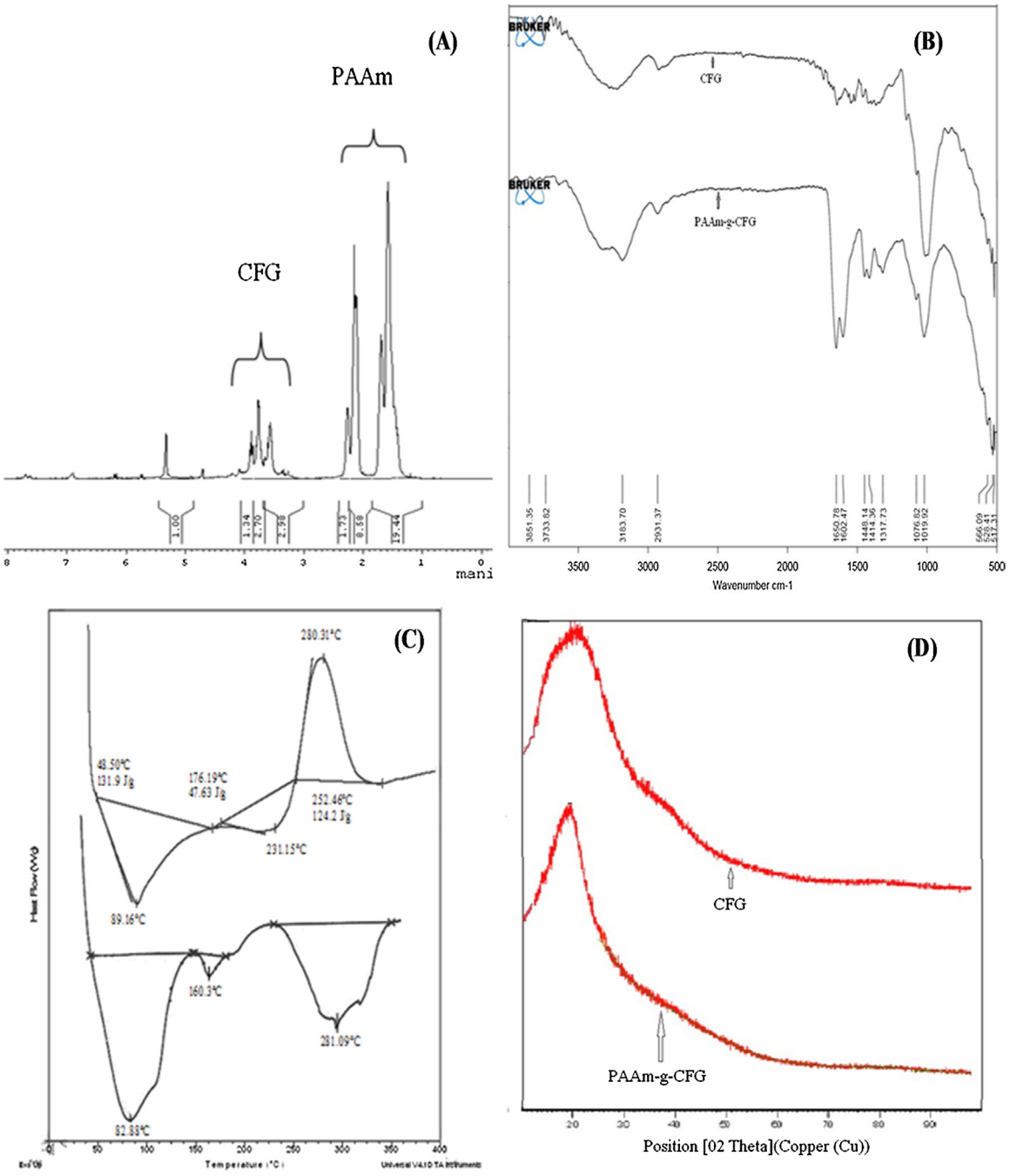

Fig. 2. Spectral and thermal attributes of CFG and PAAm-g-CFG (A) ^{1}HNMR (B) ATR-FTIR (C) DSC thermogram (D) XRD.

The mass spectra of PAAm-*g*-CFG showed different peaks at *m*/*z* ratio of different fragments of grafted copolymer. Seven Peaks are separated and different fragments were identified. The *m*/*z* ratio at 9385.392, 1462.462, 1330.332, 1209.23, 700.706, 609.63 and 467.47 suggested the presence of different acrylamide units in different fragments of grafted copolymer. The spectra depicted that acrylamide unit mainly attach to alkoxy group of different xylopyranose backbone of CFG suggesting successful grafting of polyacrylamide on CFG. The result of all the fragments appears in the mass spectra of PAAm-*g*-CFG is summarized in Table 2. Thus, the molecular weight of PAAm-g-CFG was found to be 9385.592 *m*/*z* i.e. the molecular weight of largest fragment obtained by reframing all the fragments.

3.4. Morphological analysis

The scanning electron micrographs of CFG particles show amorphous (Fig. 3A) nature and SEM images of PAAm-*g*-CFG (Fig. 3B) show that the grafting of monomer onto CFG brings about the change in the shape and size of the CFG particles. Further, it is evident from the image that the particles of PAAm-*g*-CFG are bigger in size than CFG.

3.5. Gel strength

The gel strength was estimated using TTC spreadability probe of texture analyser which showed increase in firmness with the increase in concentration of PAAm-*g*-CFG or CFG. Work of shear

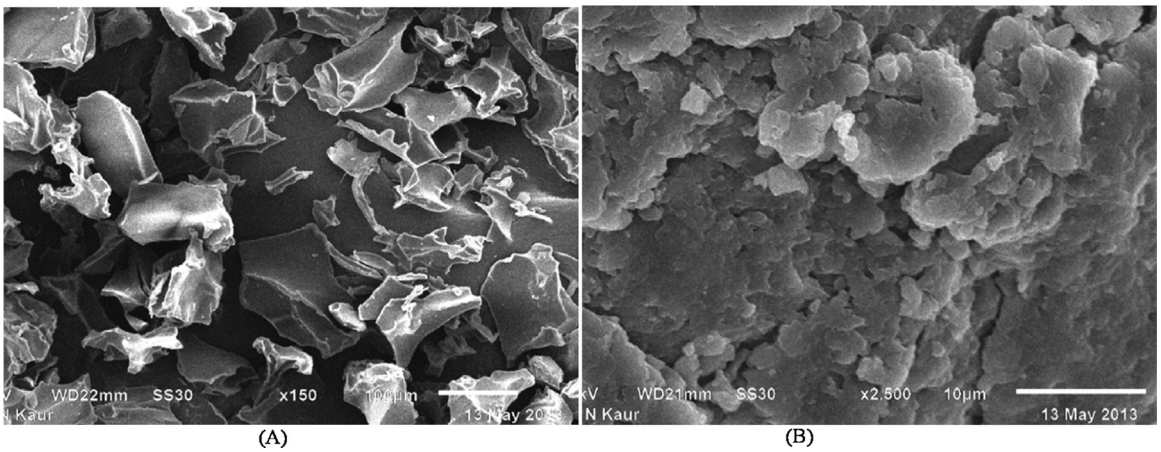

Fig. 3. SEM images of (A) CFG; (B) PAAm-g-CFG.

is the mean area of force vs time plot obtained during firmness studies. The positive sign of work of shear indicated work of cohesion (i.e. PAAm-g-CFG particle to particle strength) and negative sign of work of shear indicated work of friction (i.e. PAAm-g-CFG particles to probe surface detachment strength). The positive magnitude of work of shear of PAAm-g-CFG as compared to putative form suggested enhanced strength of PAAm-g-CFG in terms of surface behaviour. In addition, firmness is a measure of the maximum force required to extrude a sample from concentric annular space between plunger and container. Thus, maximum firmness and positive magnitude of work of shear could be considered as the good characteristics of PAAm-g-CFG. However, the work of shear was found to decrease with increase in concentration of PAAm-*g*-CFG. The back extrusion rig probe attachment provides firmness, consistency, cohesiveness and index of viscosity. The maximum positive force of extrusion (firmness (N)), area of curve (consistency (N.s)), maximum negative force due to back extrusion (cohesiveness (N)) and the negative area of extrusion (index of viscosity (N.s)) were documented as descriptors of rheological behaviour of samples. The firmness is peak or maximum force. The higher the value, firmer is the sample. The area of curve up to this point is taken as measurement of consistency. Higher the value, thicker is the consistency of the sample. The maximum negative force is taken as indicator of cohesiveness of the sample. The more negative is the value, the more is cohesiveness of sample. The mean area of negative region of the curve is work of cohesion or index of viscosity. The higher is the value, the more resistance to withdraw the probe (Sharma et al., 2015). Hence, the samples with increasing viscosity exhibited greater firmness, consistency, cohesiveness and index of viscosity (Table 3). The results indicated CFG (5–10% w/v) has high index of viscosity, cohesiveness and firmness when compared with PAAm-*g*-CFG (5–10% w/v) and HPMC K4M (2.5% w/v). However, PAAm-*g*-CFG showed enhanced consistency in comparison to CFG as well as HPMC K4M (2.5% w/v). Thus, the results revealed firmness, cohesiveness and index of viscosity follows the order CFG (5–10% w/v) > PAAm-*g*-CFG (5–10% w/v) > HPMC K4 M (2.5% w/v) whereas the consistency follows the order PAAm-*g*-CFG (5–10% w/v) > CFG (5–10% w/v) > HPMC K4 M (2.5% w/v). This suggested polyacrylamide derivatization increase gelling behaviour of CFG. Further, the lower magnitude of firmness obtained using TTC spreadability attachment of texture analyser as compared to firmness obtained by back extrusion rig was found to be due to enhanced consistency of PAAm-*g*-CFG.

3.6. Mucoadhesive strength

The results of mucoadhesive potential of PAAm-*g*-CFG as compared to CFG are summarized in Table 3. The results suggested 2.4 fold enhancement of mucoadhesive strength (Adhesive force with respect to tissue) of PAAm-*g*-CFG w.r.t. porcine gastric mucosa and around 1.6 fold enhancement of mucoadhesive strength w.r.t. mucin (2% w/v solution in PBS pH 7.4). Deshmukh, Jadhav, and Sakarkar (2014) prepared mucoadhesive theophylline tablets using karaya gum (45% w/w), locust bean gum (45% w/w), xan-

Table 3
Gel strength and mucoadhesive profile of PAAm-g-CFG.

Batch Code	Conc. of polymer	TTC Spreadability probe		Back extrusion rig			
		Firmness (N) (Probe)	Work of shear (Ns)*10^{-2}	Firmness (N)	Consistency (N s)*10^{1}	Cohesiveness (N)	Index of viscosity (N s)
D1	PAAm-g-CFG-5%	7.39 ± 0.37	7.6 ± 0.30	14.12 ± 0.5	7.712 ± 1.34	−9.7 ± 0.56	−4.38 ± 0.21
D2	PAAm-g-CFG-8%	8.288 ± 0.39	5.4 ± 0.50	16.34 ± 0.6	7.943 ± 2.01	−11.23 ± 0.67	−4.82 ± 0.13
D3	PAAm-g-CFG-10%	10.41 ± 0.47	4.5 ± 0.80	17.62 ± 0.5	10.017 ± 1.4	−13.45 ± 0.6	−5.00 ± 0.11
G1	CFG-5%	6.49 ± 0.32	7.3 ± 1.2	17.09 ± 0.7	5.4439 ± 1.7	−15.59 ± 0.45	−6.20 ± 0.13
G2	CFG-8%	6.98 ± 0.23	4.4 ± 0.34	20.08 ± 0.7	7.336 ± 1.23	−16.26 ± 1.23	−7.0.0 ± 0.9
G3	CFG-10%	7.67 ± 0.21	3.9 ± 0.45	31.832 ± 69	9.514 ± 2.13	−17.41 ± 0.4	−8.40 ± 0.23
H1	HPMC K4M-2.5%	–	–	13.3 ± 0.38	4.35 ± 1.65	−8.4 ± 0.63	−0.75 ± 0.32

Mucoadhesive strength (g)

S. No	Sample	Mucoadhesive strength (g)	
		Porcine Gastric Mucosa	Mucin (2% w/v solution)
1.	CFG	10.13 ± 1.12	372.91 ± 2.49
2.	PAAm-g-CFG	24.68 ± 2.24	596.69 ± 3.01
3.	Acrylamide	2.94 ± 0.72	–

Table 4
Rotational Rheological level approach for CFG and PAAm-g-CFG.

S.No.	Sample	ηeff (100 s^{-1}) (Pa s)	Controlled Shear Rate			Controlled Shear Stress				Behaviour
			Power Law Model			Herschel Bulkley model				
			K(Pa s^n)	n	R^2	τo (Pa)	kH (Pa s^n)	nH	R^2	
1.	10% w/v CFG	0.0328	0.15	0.72	0.99	3.47	0.24	0.87	0.99	Shear thinning
2.	20% w/v CFG	1.04	0.99	1.01	0.99	3.67	1.34	0.95	0.99	Shear thinning
3.	10% w/v PAAm-g- CFG	0.183	0.18	1.00	0.99	3.45	0.33	0.87	0.99	Shear thinning
4.	20% w/v PAAm-g- CFG	2.1	2.51	0.96	0.99	4.82	2.44	0.96	0.99	Shear thinning

than gum (45% w/w) and guar gum (45% w/w) alone and found 23.95 ± 0.36 g, 18.96 ± 0.24 g, 23.13 ± 0.95 g and 23.41 ± 0.57 g mucoadhesion respectively, using porcine gastric mucosa which is lower than PAAm-*g*-CFG. Azhar, Kumar, Sood, and Shyale (2012) examined mucoadhesive strength of gelatin (5–10% w/w), chitosan (5–10% w/w) and xanthan gum (5–10% w/w) to prepare mucoadhesive ondansetron hydrochloride tablet. They reported 9.667 ± 0.115 to 12.133 ± 0.208 g, 15.200 ± 0.45 to 17.567 ± 0.115 g and 20.933 ± 0.404 to 23.00 ± 0.500 g mucoadhesive strength using sheep buccal mucosa respectively, for gelatin (5% to 10% w/w), chitosan (5–10% w/w) and xanthan gum (5–10% w/w) (Azhar et al., 2012). Further, the mucoadhesive property of Moringa Oleifera (6% and 8% w/w) using porcine intestinal mucosa was also found to be 15.39 ± 0.98 g to 19.97 ± 0.89 g respectively i.e. lower than PAAm-*g*-CFG (Patel, Patel, & Upadhyay, 2012). Overall, to examine the position of PAAm-*g*-CFG on mucoadhesion scale w.r.t. porcine gastric mucosa, following order was obtained: PAAm-*g*-CFG > Karaya gum (45% w/w) > Guar gum (45% w/w) > Xanthan gum (45% w/v) > Locust beam gum (45% w/w) > CFG. However, the position of PAAm-g-CFG on mucoadhesion scale with respect to other mucin containing tissue, follows order: PAAm-g-CFG > Xanthan gum (10% w/w) > Xanthan gum (5% w/w) > Moringa Oleifera (8% w/w) > Chitosan (10% w/w) > Moringa Oleifera (6% w/w) > Chitosan (5% w/w) > Gelatin (10% w/w) > CFG > Gelatin (5% w/w).

3.7. Rheological performance

The rheological performance of PAAm-*g*-CFG was studied at different rotational levels and oscillatory rheological level. The two commonly applied approaches to study rotational rheological behaviour are either at controlled shear rate (CSR) and controlled shear stress (CSS) approach. In both the approaches, 10% w/v and 20% w/v solution was placed between two plates. In the CSR approach, torque produced was measured at applied speed. In the CSS approach, angular speed produced was measured at applied torque and this approach was reported to be better approach for yield stress determination (Moller, Mewis, & Bonn, 2006) because the variable of primarily interest can be carefully controlled. Therefore, for determination of yield stress, CSS approach was used.

The power law and Herschel-Bulkley model was applied that confirms positive value of "n" indicating plastic flow (less pseudoplastic) nature of both CFG and PAAm-*g*-CFG (Table 4). The power law model is an easy to use model that is ideal for plastic as well as pseudoplastic materials relatively mobile fluids such as weak gels and low viscosity dispersions. The equation for the model is

$$\text{Shearstress} = k(\text{shearrate})^n$$

Where, 'k' is the consistency coefficient (Pa S) and exponent 'n' is the flow index that reflects closeness to newtonian flow. The higher value of 'k' for PAAm-*g*-CFG compared with those of CFG (irrespective of their concentration) indicates polyacrylamide grafting on CFG enhanced viscosity. Further, the decrease in value of 'k' with decrease in concentration of either polysaccharide reflects decrease in consistency index. The exponent 'n' i.e. flow index was found to be close to 1 suggesting less pseudoplastic character of PAAm-*g*-CFG (Fig. 4A–D). Further, when yield stress of material is measurable, it can be included in the power law model and that model become Herschel Bulkley model:

$$(\text{Shearstress}) - (\text{Yieldstress}) = k_H(\text{Shearrate})^{nH}$$

The k_H and n_H are consistency index and flow behaviour index, respectively.

When the experiments were conducted at CSS approach, the occurrence of yield stress suggested both CFG and PAAm-*g*-CFG exhibited Herschel Bulkley behaviour, because of existence of yield point (τ_o). Further, the 1.31 fold enhancement in τ_o was evident when CFG (20% w/v) was derivatized to PAAm-*g*-CFG (20% w/v), indicating the increase in structural stability. Tipvarakarnkoon and Senge (2008) reported lower 'n' value (0.186) and high 'k' value (12.460 Pa s^n) for xanthan gum (1% w/v) suggesting high structural stability as compared to PAAm-*g*-CFG (20% w/v). However, PAAm-*g*-CFG bear higher structural stability when compared with cordia gum (4% w/v) with 'n' value 1.06, 'k' value 0.036 and showed newtonian behaviour at 50 °C with lower consistency index (Rafe & Masood, 2014). Thus, the position of PAAm-*g*-CFG on basis of their structural stability and pseudoplastic character are: 1% xanthan > 10% CFG and PAAm-*g*-CFG > 20% CFG > 20% PAAm-*g*-CFG > cordia abyssinica gum.

In addition, the apparent viscosities at relatively high shear rate, 100 s^{-1} (η_{eff}) was two times higher for PAAm-*g*-CFG (20% w/v) as compared to CFG (20% w/v) (Table 4) suggesting polymerization leads to structural stability (Tipvarakarnkoon & Senge, 2008).

Viscoelastic analysis of CFG and PAAm-*g*-CFG was described using G′ (storage modulus), G″ (loss modulus) and tan δ at amplitude sweep approach and frequency-sweep approach. The amplitude sweep approach was applied to determine LVR (linear viscoelastic region). The results suggested 10% strain for LVR was suitable for both CFG 10% w/v and 20% w/v, whereas 10% and 5% strain in the LVR, respectively for PAAm-*g*-CFG 10% w/v and 20% w/v solutions. The results suggested G″ > G′ for CFG (10% or 20% w/v) and PAAm-*g*-CFG (10% or 20% w/v) indicating liquid like viscous liquid.

In the frequency domain 10^{-1}–10^{1} s^{-1}, the PAAm-*g*-CFG behaves as a structured compound with the viscous and elastic modulus evolving in parallel and the liquid state predominant (G″ > G′). Further, the polyacrylamide derivatization of CFG leads to more viscous like nature as evident from the difference between G″ to G′ (Fig. 4E–H). The complex viscosity (η^*) decreases for all analysed solution during the treatment at low frequency. Complex viscosity (η^*) increases when frequency decrease indicating some structural stability, which could be correlated with increase in molecular weight and chain length for PAAm-g-CFG as compared to CFG. This could be evident from the appearance of turning point in a plot of η^* vs ω that attires value around 10 rad/s. These samples of PAAm-g-CFG have fewer turning points as compared to the CFG (Fig. 4E–H). This may probably be due to the high structural stability of PAAm-g-CFG.

The temperature sweep studies from 10 °C to 80 °C and 80 °C to 10 °C shown in Fig. 4(I–J) i.e. heating/cooling cycle follows

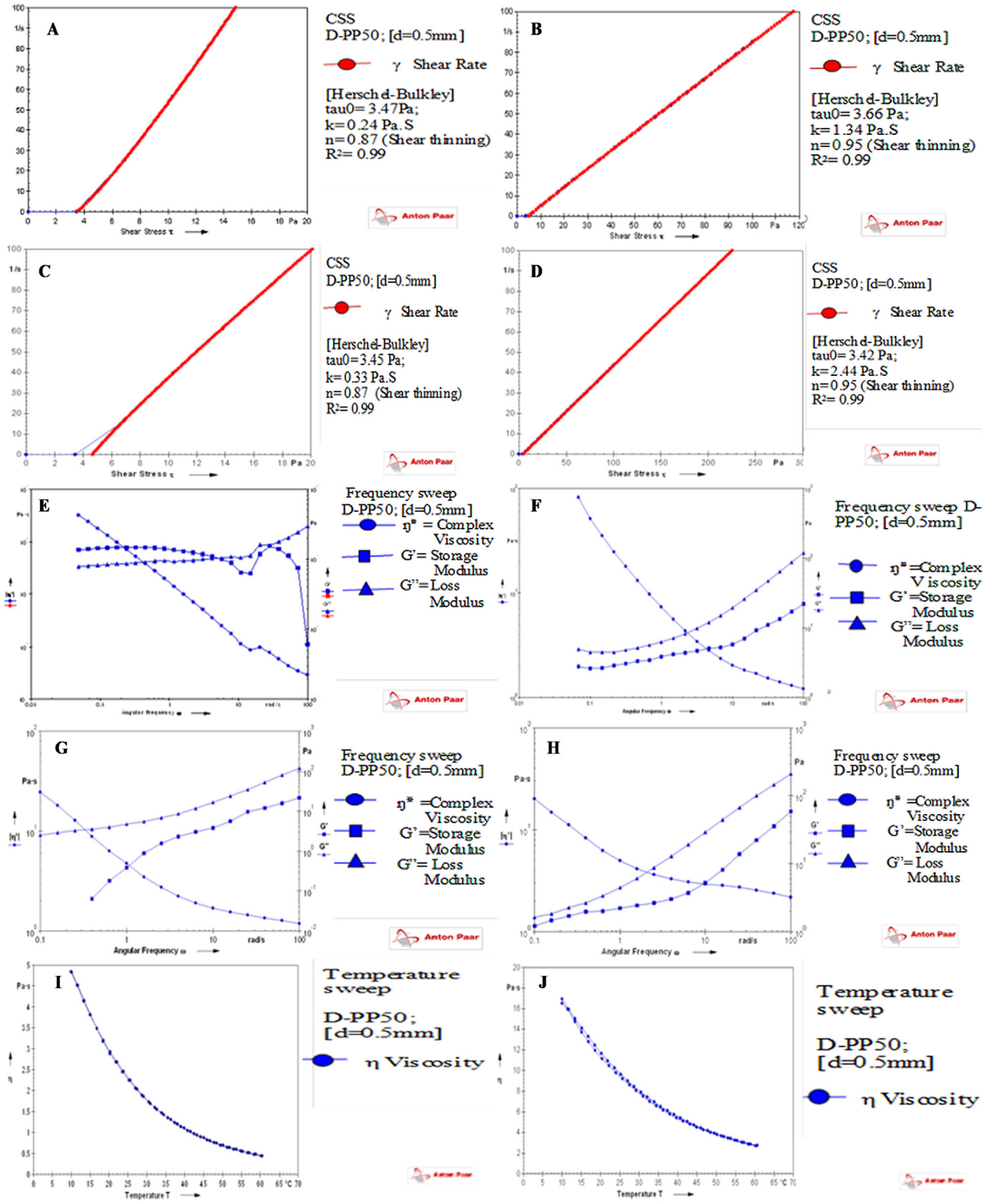

Fig. 4. Rheogram generated at controlled shear rate approach between shear stress-shear rate (A) 10% CFG (B) 20% CFG (C) 10% PAAm-g-CFG (D) 20% PAAm-g-CFG; Frequency sweep approach between η^* vs ω (E) 10% CFG (F) 20% CFG (G) 10% PAAm-g-CFG (H) 20% PAAm-g-CFG; Temperature sweep approach (I) 20% CFG (J) 20% PAAm-g-CFG.

Arrhenius equation at 25 °C showing $R^2 = 0.99$ for both CFG and PAAm-g-CFG. The activation energy (E_a) for CFG was 76.799 KJ/mol lower than 105.34 KJ/mol for PAAm-g-CFG suggests high temperature stability. The higher value of E_a i.e. 105.34 KJ/mol in case of 20% w/v PAAm-g-CFG shows it could maintain its viscosity at higher temperature. A similar finding were reported for xanthan gum having E_a of 5.74 KJ/mol which maintain its viscosity at higher temperature more than Cordia gum bearing E_a of 4.323 KJ/mol at shear rate 100 s^{-1} (Rafe & Masood, 2014). The order of polysaccha-

rides on the basis of E_a indicate thermal stability as follow, Cordia gum < Xanthan gum < CFG < PAAm-*g*-CFG.

In another study, Ea was found to be increased with increase in proportion of isabgol husk in a combination of isabgol:gum katira (25:75 to 75:25) (Sharma, Mazumder, & Nautiyal, 2014) suggesting isabgol provide thermal stability to system. Thus, comparing thermal stability of PAAm-*g*-CFG suggested isabgol > PAAm-*g*-CFG > gum katira.

Overall, the rheological analysis of PAAm-*g*-CFG suggested shear thinning behaviour and liquid like viscous fluid having high chemical and thermal stability additive.

4. Conclusion

The graft copolymer of corn fibre gum was successfully synthesized employing quality by design approach. The technique suggested 5 g acrylamide, 0.4 g ammonium persulfate (initiator) and 80 °C temperature was necessary to obtain pure PAAm-*g*-CFG with 552 ± 2.4% grafting and 6.52 ± 0.34% yield and 110 ± 2.8% grafting efficiency. Further, the synthesized grafted copolymer bears highest mucoadhesive strength as compared to moringa oleifera gum, karaya gum, guar gum, xanthan gum, chitosan and gelatin suggesting high pharmaceutical benefits. In addition, the PAAm-*g*-CFG behaves as shear thinning liquid that follows Herschel Bulkley model. The viscoelastic analysis pointed towards liquid like viscous liquid nature of PAAm-*g*-CFG, indicating its application to food as well as pharmaceutical industry.

Acknowledgement

The author would like to acknowledge the financial assistance provided by AICTE, RPS (project no. 8-188/RIFD/RPS/POLICY-1/2014-15).

References

Adhikary, P., & Krishnamoorthi, S. (2013). Microwave assisted synthesis of polyacrylamide grafted amylopectin. *Materials Research Innovations*, *17*(2), 67–72.

Al-Karawi, A. J. M., Al-Qaisi, Z. H. J., Abdullah, H. I., Al-Mokaram, A. M. A., & Al-Heetimi, D. T. A. (2011). Synthesis, characterization of acrylamide grafted chitosan and its use in removal of copper (II) ions from water. *Carbohydrate Polymers*, *83*(2), 495–500.

Azhar, S. A., Kumar, P. R., Sood, V., & Shyale, S. (2012). Studies on directly compressed Ondansetron hydrochloride mucoadhesive buccal tablets using chitosan, gelatin & xanthan gum along with HPMC K4 M. *Journal of Applied Pharmaceutical Science*, *2*(5), 100–105.

Behari, K., Pandey, P. K., Kumar, R., & Taunk, K. (2001). Graft copolymerization of acrylamide onto xanthan gum. *Carbohydrate Polymer*, *46*(2), 185–189.

Cao, Y., Qing, X., Sun, J., Zhou, F., & Lin, S. A. (2002). Graft copolymerization of acrylamide onto carboxymethyl starch. *European Polymer Journal*, *38*(9), 1921–1924.

Darmayanti, M. G., & Radiman, C. L. (2015). Synthesis and characterization of kappa-carrageenan-graft-acrylamide for enhanced oil recovery application. *Polymer-Plastics Technology and Engineering*, *54*(3), 259–264.

da Silva, D. A., de Paula, R. C., & Feitosa, J. P. (2007). Graft copolymerisation of acrylamide onto cashew gum. *European Polymer Journal*, *43*(6), 2620–2629.

Deshmukh, V. N., Jadhav, J. K., & Sakarkar, D. M. (2014). Formulation and *in-vitro* evaluation of theophylline anhydrous bioadhesive tablets. *Asian Journal of Pharmaceutics*, *3*(1), 54–58.

Durcilene, A., Regina, C. M., & Judith, P. A. (2007). Graft copolymerization of acrylamide onto cashew gum. *European Polymer Journal*, *43*(6), 2620–2629.

Gowrav, M. P., Umme, H., Hosakote, G. S., Riyaz, A. M., & Srivastava, A. (2015). Polyacrylamide grafted guar gum based glimepiride loaded pH sensitive pellets for colon specific drug delivery: Fabrication and characterization. *Royal Society of Chemistry Advances*, *5*(97), 80005–80013.

Gupta, S., Madan, R. N., & Bansal, M. C. (1987). Chemical composition of *Pinus caribaea* hemicellulose. *Tappi Journal*, *70*, 113–114.

Jiang, F. T., Li, W. F., Zhan, X. H., Chen, G. F., Zhou, J., & Huang, J. (2006). Preparation and characterization of Konjac superabsorbent polymer. *Journal of Wuhan University Technology-Material Science Education*, *21*(4), 87–91.

Jindal, M., Rana, V., Kumar, V., Sapra, B., & Tiwari, A. K. (2013). Synthesis, physico-chemical and biomedical applications of sulfated Aegle marmelos gum: Green chemistry approach. *Arabian Journal of Chemistry*.

Kamboj, S., & Rana, V. (2014). Physicochemical: Rheological and antioxidant potential of corn fibre gum. *Food Hydrocolloids*, *39*, 1–9.

Kurkuri, M. D., Kumbar, S. G., & Aminabhavi, T. M. (2002). Synthesis and characterization of polyacrylamide-grafted sodium alginate copolymeric membranes and their use in pervaporation separation of water and tetrahydrofuran mixtures. *Journal of Applied Polymer Science*, *86*(2), 272–281.

Maia, M. S., Silva, V. M., Curti, P. S., & Balaban, R. C. (2012). Study of the reaction of grafting acrylamide onto xanthan gum. *Carbohydrate Polymer*, *90*(2), 778–783.

Mishra, A., & Bajpai, M. (2005). Synthesis and characterization of polyacrylamide grafted copolymers of kundoor mucilage. *Journal of Applied Polymer Science*, *98*(3), 1186–1191.

Mishra, A., Bajpai, M., & Pandey, S. (2006). Removal of dyes by biodegradable flocculants: A lab scale investigation. *Seperation Science and Technology*, *41*(3), 583–593.

Mishra, A., Bajpai, M., Pal, S., Agrawal, M., & Pandey, S. (2006). Tamarindus indica mucilage and its acrylamide-grafted copolymer as flocculants for removal of dyes. *Colloid and Polymer Science*, *285*(2), 161–168.

Moller, P. C., Mewis, J., & Bonn, D. (2006). Yield stress and thixotropy: On the difficulty of measuring yield stresses in practice. *Soft Matter*, *2*(4), 274–283.

Mundargi, R. C., Patil, S. A., & Aminabhavi, T. M. (2007). Evaluation of acrylamide-grafted-xanthan gum copolymer matrix tablets for oral controlled delivery of antihypertensive drugs. *Carbohydrate Polymers*, *69*(1), 130–141.

Patel, M. T., Patel, J. K., & Upadhyay, U. M. (2012). Assessment of various pharmaceutical excipient properties of natural Moringa Oleifera gum. *International Journal of Pharmacy & Life Science*, *3*(7), 1833–1847.

Pledger, H., Jr., Young, T. S., Wu, G. S., Butler, G. B., & Hogen-Esch, T. E. (1986). Synthesis and characterization of water-soluble starch-acrylamide graft copolymers. *Journal of Macromolecular Science—Chemistry*, *23*(4), 415–436.

Rafe, A., & Masood, H. S. (2014). The rheological modeling and effect of temperature on steady shear flow behaviour of Cordia abyssinica Gum. *Journal of Food Processing and Technology*, *5*, 309.

Rani, P., Sen, G., Mishra, S., & Jha, U. (2012). Microwave assisted synthesis of polyacrylamide grafted gum ghatti and its application as flocculant. *Carbohydrate Polymers*, *89*(1), 275–281.

Sanghi, R., Bhattacharya, B., & Singh, V. (2006). Use of Cassia javahikai seed gum and gum g-polyacrylamide as coagulant aid for the decolorization of textile dye solutions. *Bioresources Technology*, *97*(10), 1259–1264.

Sharma, B. R., Kumar, V., & Soni, P. L. (2002). Ceric ammonium nitrate-initiated graft copolymerization of acrylamide onto Cassia tora gum. *Journal of Applied Polymer Science*, *86*(13), 3250–3255.

Sharma, K. V., Mazumder, B., & Nautiyal, V. (2014). Rheological characterization of isabgol husk, gum katira hydrocolloids, and their blends. *International Journal of Food Science*, 1–10.

Sharma, R., Kamboj, S., Khurana, R., Singh, G., & Rana, V. (2015). Physicochemical and functional performance of pectin extracted by QbD approach from *Tamarindus indica* L pulp. *Carbohydrate Polymer*, *134*, 364–374.

Singh, V., Tiwari, A., Tripathi, D. N., & Sanghi, R. (2004). Microwave assisted synthesis of Guar-g-polyacrylamide. *Carbohydrate Polymer*, *58*(1), 1–6.

Singh, V., Kumar, P., & Sanghi, R. (2012). Use of microwave irradiation in the grafting modification of the polysaccharide—A review. *Progress in Polymer Science*, *37*(2), 340–364.

Sun, R. C., Fang, J. M., Tomkinson, J., & Jones, G. L. (1999). Acetylation of wheat straw hemicellulose in N,N-dimethylacetamide: LiCl solvent system. *Industrial Crops and Products*, *10*(3), 209–218.

Tame, A., Ndikontar, M. K., Ngamveng, J. N., Ntede, H. N., Mpon, R., & Njungab, E. (2011). Graft copolymerisation of acrylamide on carboxymethyl cellulose (CMC). *Rasayan journal of chemistry*, *4*(1), 1–7.

Tipvarakarnkoon, T., & Senge, B. (2008). Rheological behaviour of gum solutions and their interaction after mixing. *Annual Transactions of the Nordic Rheology Society*, *16*, 73–80.

Toti, U. S., & Aminabhavi, T. M. (2004). Modified guar gum matrix tablet for controlled release of diltiazem hydrochloride. *Journal of Controlled Release*, *95*, 567–577.

Xu, F., & Sun, R. C. (2004). Analysis and characterization of acetylated sugarcane bagasse hemicellulose. *International Journal of Polymer Analysis and Characterization*, *9*(4), 229–244.

Yadav, M. P., Johnston, D. B., & Hicks, K. B. (2007). Structural characterization of Corn fibre gum coarse and fine fibre and a study of their emulsifying properties. *Journal of Agricultural and Food Chemistry*, *55*(15), 6366–6371.

Yadav, M. P., Johnston, D. B., & Hicks, K. B. (2009). Corn fibre gum: New structure/function relationship for this potential beverages flavour stabilizer. *Journal of Food Hydrocolloids*, *23*(6), 1488–1493.